

Structure and excited state dipole moments of oxygen containing heteroaromatics: 2,3-benzofuran



Marie-Luise Hebestreit ^{a,*}, Hilda Lartian ^a, Michael Schneider ^a, Ralf Kühnemuth ^b, América Yareth Torres-Boy ^c, Sergio Romero-Servin ^c, José Arturo Ruiz-Santoyo ^c, Leonardo Alvarez-Valtierra ^c, W. Leo Meerts ^d, Michael Schmitt ^a

^a Heinrich-Heine-Universität, Institut für Physikalische Chemie I, D-40225, Düsseldorf, Germany

^b Heinrich-Heine-Universität, Lehrstuhl für Molekulare Physikalische Chemie, D-40225, Düsseldorf, Germany

^c División de Ciencias e Ingenierías, Universidad de Guanajuato-Campus León, León, Guanajuato, 37150, Mexico

^d Radboud University, Institute for Molecules and Materials, Felix Laboratory, Toernooiveld 7c, 6525, ED, Nijmegen, the Netherlands

ARTICLE INFO

Article history:

Received 31 December 2019

Received in revised form

19 February 2020

Accepted 29 February 2020

Available online 6 March 2020

Dedicated to the memory of Jon Hougen.

Keywords:

2,3-benzofuran

Coumarone

benzo[b]furan

Rotational spectrum

Excited state

Dipole moment

TCSPC

ABSTRACT

The rotationally resolved electronic spectra of the origin band of 2,3-benzofuran has been measured and analyzed. Using electronic Stark spectroscopy, the dipole moments in the ground and electronically excited state have been determined. From the values for the permanent dipole moments, the orientation of the transition dipole moment and from the geometry changes upon excitation, the lowest excited singlet state could be shown to be of 1L_b symmetry. These results are compared to those of indole in particular. Moreover, the excited state lifetime of isolate 2,3-benzofuran in the gas phase has been determined to be 14 ns and compared to the excited state lifetime of 2,3-benzofuran in ethylacetate solution of 4 ns

© 2020 The Authors. Published by Elsevier B.V. This is an open access article under the CC BY-NC-ND license (<http://creativecommons.org/licenses/by-nc-nd/4.0/>).

1. Introduction

The electronically excited states of indole, the chromophore of the aromatic amino acid tryptophan have been scrutinized over many decades. However, its oxygen (coumarone, 2,3-benzofuran, benzo [b]furan), sulfur (thionaphthene, benzo [b]thiophene) and carbon (indene) analogues have been studied much less.

Phenyl-substituted benzofurans have been studied as efficient inhibitors for chloride channel proteins (CLC-K), depending on the conformation of the phenyl ring with respect to the benzofuran moiety [1]. Furthermore, benzofuran derivatives are used as anti-arrhythmic drugs with sodium channel blocking activity [2]. Recently, 6-(2-aminopropyl)benzofuran has found considerable interest as serotonin-norepinephrine-dopamine reuptake inhibitor

with empathogenic psychoactive effects [3].

Much work on indole and its derivatives was dedicated to their photophysical properties, which are governed by the existence of two close-lying electronically excited singlet states. There are numerous theoretical contributions to the photophysical properties of indole excited states [4–11]. Experimental work using rotationally resolved electronic spectroscopy in the gas phase [12–14] and two-photon fluorescence excitation spectroscopy [15] proofed that the lowest excited state of isolated indole is the L_b -state. Clusters of indole with polar molecules also have the L_b -state as lowest excited singlet state [13,16], while for substituted indoles both L_b - [17–21] as well as the L_a -state [22–27] have been found as lowest singlet states.

Platt [28] derived a scheme for labeling the lowest electronically excited states of cata-concatenated hydrocarbons as 1L_b - and 1L_a -states. This nomenclature has been extended to the case of the unsymmetric molecule indole by Weber [29]. Due to its lower molecular symmetry, the two states belong to the same

* Corresponding author.

E-mail address: Marie-Luise.Hebestreit@uni-duesseldorf.de (M.-L. Hebestreit).

representation and can only be distinguished by their spectral signatures. Moreover, the states are assumed to be close in energy and, therefore, are strongly coupled. The electronic transition dipole moments (TDM) for excitation from the electronic ground state to the $^1\text{L}_b$ - and $^1\text{L}_a$ -states are oriented differently. For many indole derivatives, they are nearly orthogonal to each other [30]. The $^1\text{L}_a$ -state is very polar and, therefore, its energy depends strongly on the polarity of its solvent environment, whereas this is typically not the case for $^1\text{L}_b$.

The vibronic spectrum of 2,3-benzofuran has been measured and analyzed by Hollas [31]. A rotational contour of the electronic origin bands of 2,3-benzofuran and its sulfur analogue thionaphthene have been presented by the Lombardi group [32]. The Levy group performed fluorescence excitation, dispersed fluorescence and resonantly enhanced two-photon ionization (RE2PI) techniques on 2,3-benzofuran, dibenzofuran and fluorene [33]. The Pratt group has studied, using high resolution laser induced fluorescence spectroscopy (HRLIF), fluorene, carbazole, dibenzofuran [34] and dibenzothiophene [35]. Collier gave a full vibrational assignment of the infrared and Raman spectra of 2,3-benzofuran in the gas phase from a comparison to a normal mode analysis with the AM1 force field [36]. An improved vibrational assignment of the gas and liquid phase FTIR and Raman spectra was published later by Klots and Collier [37]. Smithson *et al.* deduced the coplanarity of the benzene and furan rings from far-infrared spectroscopy [38]. *Ab initio* quantum chemical calculations of the total energy, ionization potential and dipole moments have been given by Palmer and Kennedy [39].

In the present contribution we will analyze the changes of geometry and dipole moments upon electronic excitation of 2,3-benzofuran.

2. Experimental section

2.1. Experimental procedures

2.1.1. Rotationally resolved electronic (Stark) spectroscopy

2,3-benzofuran ($\geq 99\%$) was purchased from Sigma Aldrich. The sample was used without further purification and heated to $80\text{ }^\circ\text{C}$ and co-expanded with 200–300 mbar of argon through a 147 μm nozzle into the vacuum. The molecular beam was formed by co-expanding in the molecular beam machine consisting of three differentially pumped vacuum chambers by using two skimmers (1 mm and 3 mm) linearly aligned inside the machine. 360 mm downstream of the nozzle the molecular beam was crossed with the laser beam at right angles. A single frequency ring dye laser (Sirah Matisse DS) operated with Rhodamine 110 was pumped by 10 W of the 532 nm line of a diode pumped solid state laser (Spectra-Physics Millennia eV) to create the excitation beam. The fluorescence light of the dye laser, centered at 17975 cm^{-1} with 570 mW of power, was frequency doubled in an external folded ring cavity (Spectra Physics Wavetrain) with a resulting power of about 4 mW during the experiments. The fluorescence of the sample was collected perpendicular to the plane defined by laser and molecular beam by a light collecting system consisting of a concave mirror and two planoconvex lenses onto the photocathode of a UV enhanced photomultiplier tube (Thorn Emi 9863QB). For data recording and processing the signal output was discriminated and digitized by a photon counter and transmitted to a PC. The relative frequency was determined using a *quasi* confocal Fabry-Perot interferometer and the relative frequency was obtained by comparing the recorded spectrum to the tabulated lines in the iodine absorption spectrum [40]. A detailed description of the experimental setup for

rotationally resolved laser induced fluorescence spectroscopy has been given previously [41,42]. The effective distance of the Stark plates is 23.49 ± 0.05 mm, calibrated using the accurately known dipole moment of benzonitrile [20,43]. They consist of a parallel pair of electro-formed nickel wire grids (18 mesh per mm, 50 mm diameter) with a transmission of 95% in the UV. The polarization plane of the incoming laser beam can be rotated by 90° inside the vacuum chamber by means of an achromatic $\lambda/2$ plate (Bernhard Halle 240–380 nm), which can be pushed in or pulled out of the laser beam using a linear motion vacuum feedthrough. One can choose between a parallel set-up (selection rules $\Delta M = 0$) and perpendicular (selection rules $\Delta M = \pm 1$) by changing the plane of polarization.

2.1.2. Time-correlated single photon counting

Time-correlated single photon counting (TCSPC) was performed with a DeltaFlex Ultima spectrometer (HORIBA Jobin Yvon), equipped with a supercontinuum light source SuperK Extreme EXR-20 and frequency doubler SuperK Extend-UV/DUV (both NKT Photonics). The signal was recorded at 292 nm under magic angle conditions, a pulse repetition rate of 11.1 MHz, a sample temperature of $20\text{ }^\circ\text{C}$ and with excitation at 278 nm. The instrument response function (IRF, FWHM approximately 60 ps) was recorded at the excitation wavelength, using a scattering solution (Ludox) and used in the fits applying an iterative deconvolution algorithm to minimize χ^2 .

2.2. Quantum chemical calculations

Structure optimizations were performed employing a Dunning's correlation-consistent polarized valence triple zeta (cc-pVTZ) basis set from the TURBOMOLE library [44,45]. The equilibrium geometries of the electronic ground and the lowest excited singlet states were optimized using the approximate coupled cluster singles and doubles model (CC2) employing the resolution-of-the-identity (RI) approximation [46–48]. For the structure optimizations spin-component scaling (SCS) modifications to CC2 were taken into account [49]. Vibrational frequencies and zero-point corrections to the adiabatic excitation energies were obtained from numerical second derivatives using the NumForce script [50].

2.3. Fits of the rovibronic spectra using evolutionary algorithms

Evolutionary strategies are perfect tools for the automated fit of rotationally resolved spectra, even for large molecules and dense spectra [51–54]. They are a powerful tool to handle complex multi-parameter optimizations in order to find the global minimum and are inspired by evolutionary processes in nature, which are based on reproduction, mutation and selection. For our presented high resolution spectra, we used the covariance matrix adaptation evolution strategy (CMA-ES), which is described in detail elsewhere [55,56].

3. Results

3.1. Computational results

The SCS-CC2/cc-pVTZ optimized structure of 2,3-benzofuran is planar in the ground and lowest excited singlet state. The lowest excited singlet state is comprised of 43.7 % LUMO \leftarrow HOMO-1 + 25.7 % LUMO+1 \leftarrow HOMO and 18.9 % LUMO \leftarrow HOMO excitation, cf. Fig. 2, which is a strong indication for an L_b state. Another indication for the electronic character as L_b state, is the calculated

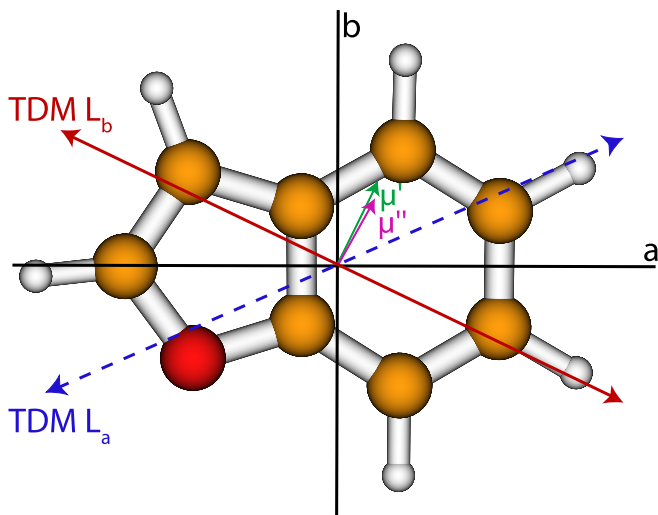


Fig. 1. Optimized ground state structure, inertial axes, transition dipole moment for excitation to the lowest excited singlet state (red, straight), and the orientation of the permanent dipole moment in the ground (magenta, straight) and first excited state (green, straight) of 2,3-benzofuran. The transition dipole moment for the excitation to the L_a -state is shown as a blue dotted arrow (only calculated). A positive sign of the angle θ_D of the dipole moment with respect to the a -axis refers to a clockwise rotation of the inertial a -axis onto the dipole/TDM vector.

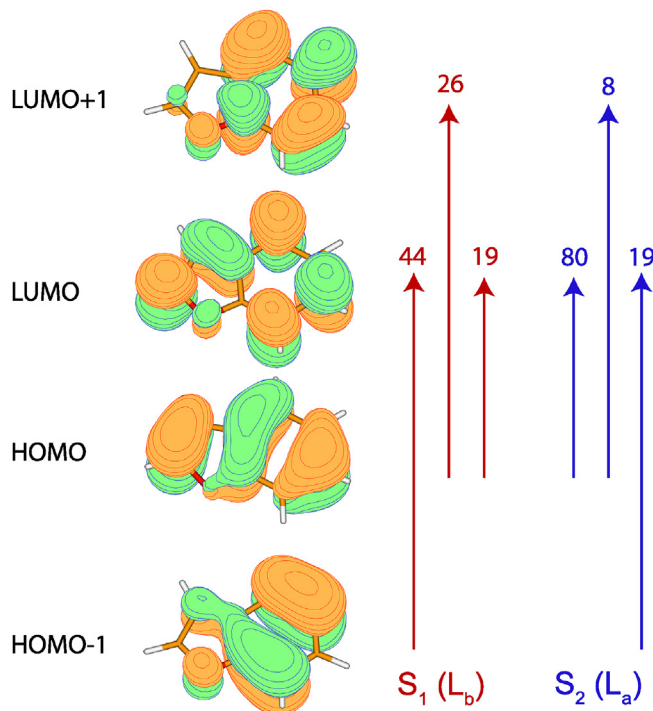


Fig. 2. Molecular orbitals of 2,3-benzofuran with the percentage of the S_1 (L_b) and S_2 (L_a) excitations according to SCS-CC2/cc-pVTZ calculations.

transition dipole moment orientation (cf. Table 1 and Fig. 1), which points away from the oxygen atom.

The molecular parameters (rotational constants A , B , and C in both electronic states, the inertial defects ΔI , the angle θ of the transition dipole moment with the inertial a -axis, the angle θ_D of the permanent dipole moment with the inertial a -axis, and the

zero-point corrected origin frequency ν_0) are compiled in Table 1 and are compared to the experimental results, which are described in detail in Section 3.2. The inertial defects¹ of 2,3-benzofuran are exactly zero for the ground and lowest excited singlet state which shows the planarity of the molecule. Since we calculate the equilibrium structure, no vibrational averaging is contained in the inertial defect, which is therefore exactly zero for a geometrically planar molecule. The calculated angle of the transition dipole moment vector for excitation to the lowest excited singlet state is $+25.3^\circ$ with respect to the inertial a -axis. The absolute value of the permanent dipole moment in the ground state is calculated to be 0.72 D and 0.86 D in the excited singlet state, with larger amounts of the b -component of the dipole vector. Not only the magnitude, but also the direction with respect to the inertial a -axis stay nearly constant.

3.2. Experimental results

Fig. 3 shows the rotationally resolved electronic spectrum of the origin of 2,3-benzofuran at 35950.01 cm^{-1} , which is set to zero on the scale of the figure. A zoomed part of the spectrum is shown in the second trace along with the best fit at zero field and in the third trace at a field strength of 2554.70 V/cm . Experimental spectra are shown as black traces, simulations, using the best fit parameters, as red traces.

As the electric field in the chosen set-up is parallel to the polarization of the plane of the exciting light, the selection rules $\Delta M = 0$ for the Stark spectrum hold. The origin is an ab -hybrid band which has predominant a -type character. From the intensities of a - and b -lines, values of 82% a and 18% b -type are calculated, resulting in an angle of the TDM with the inertial a -axis of $\pm 25.5^\circ$. The indeterminacy of the sign of the angle of $\pm 25.5^\circ$ of the TDM can be resolved by comparison to the ab initio calculated value of $+25.3^\circ$.

The fit of the molecular parameters, given in Table 1 was performed using the CMA-ES algorithm. The simulation, using the best fit parameters is shown in the red traces of Fig. 3. Very good agreement between the experimental and the simulated spectrum, based on the best fit parameters has been obtained, both for the zero-field spectrum and for the Stark spectrum at an electric field strength of 2554.70 V/cm . All lines in the zero-field spectrum are heavily split in the electric field. Note, that the two traces of zero-field and 2554.70 V/cm field in Fig. 3 cover the same spectral range.

The excited state lifetime of 2,3-benzofuran in the gas phase was obtained from the Lorentzian contribution of 10.66 MHz to the Voigt line profile using a fixed Gaussian contribution. The so determined excited state lifetime is 14.93 ns .

Additionally, lifetime measurement in ethyl acetate as solvent using TCSPC was performed. A single exponential decay is found, with a excited state lifetime of 4.4 ns . Fig. 4 presents the decay curve for 2,3-benzofuran in ethyl acetate, along with the best fit of a single exponential decay and the residue.

4. Discussion

4.1. Excited state structure

The small negative inertial defects of 2,3-benzofuran with a value of $-0.08\text{ amu}\text{\AA}^2$ for the electronic ground state and $-0.18\text{ amu}\text{\AA}^2$ for the electronically excited state, shows the planarity of the molecule for both electronic states. The slightly larger negative inertial defect of the excited state can be traced back to a zero-point

¹ The inertial defect is defined as: $\Delta I = I_a - I_b - I_c$, with the moments of inertia with respect to the inertial a , b , and c axes.

Table 1

SCS-CC2/cc-pVTZ computed and experimental molecular parameters of 2,3-benzofuran. Doubly primed parameters belong to the electronic ground and single primed to the excited state. θ_D is the angle of the permanent dipole moment vector with the main inertial a -axis. A negative sign of this angle means an anticlockwise rotation of the main inertial a -axis onto the dipole moment vector, shown in Fig. 1 θ is the angle of the transition dipole moment vector with the main inertial a -axis. The same convention for its sign is used as for θ_D . For details see text.

	Theory SCS-CC2		Theory CC2		Experiment
	L_b	L_a	L_b	L_a	
A'' /MHz	3907.51		3909.05		3921.89 (6)
B'' /MHz	1658.67		1663.75		1663.01 (2)
C'' /MHz	1164.40		1167.04		1168.04 (2)
$\Delta I''$ /amuÅ ²	0.00		0.00		-0.08
μ_a'' /D	0.43		0.30		± 0.23 (1)
μ_b'' /D	0.57		0.61		± 0.74 (1)
μ'' /D	0.72		0.68		0.77 (1)
θ_D'' °	-52.8		-63.6		± 72.7
A' /MHz	3743.23	3857.51	3747.95	3873.62	3762.26
B' /MHz	1638.90	1622.89	1644.54	1623.44	1647.61
C' /MHz	1139.84	1142.31	1143.01	1143.99	1146.30
$\Delta I'$ /amuÅ ²	0.00	0.00	0.00	0.00	-0.18
μ'_a /D	0.48	-1.31	0.35	-1.65	± 0.27 (1)
μ'_b /D	0.71	2.01	0.74	1.81	± 0.87 (1)
μ' /D	0.86	2.39	0.82	2.45	0.91 (1)
θ'_D °	-55.7	+56.9	-64.4	+47.6	± 72.8
ΔA /MHz	-164.28	-49.93	-161.1	-35.43	-159.63 (4)
ΔB /MHz	-20.67	-35.76	-19.21	-40.31	-15.39 (4)
ΔC /MHz	-24.56	-22.07	-24.03	-23.05	-21.74 (6)
$\Delta\nu_{Lorentz}$ /MHz	-	-	-	-	10.66
τ /ns	-	-	-	-	14.93
θ^o	+25.3	-22.5	+26.5	-28.3	± 25.5 (20)
ν_0 /cm ⁻¹	36651.43	41802.86	37312.66	41214.04	35950.01 (1)

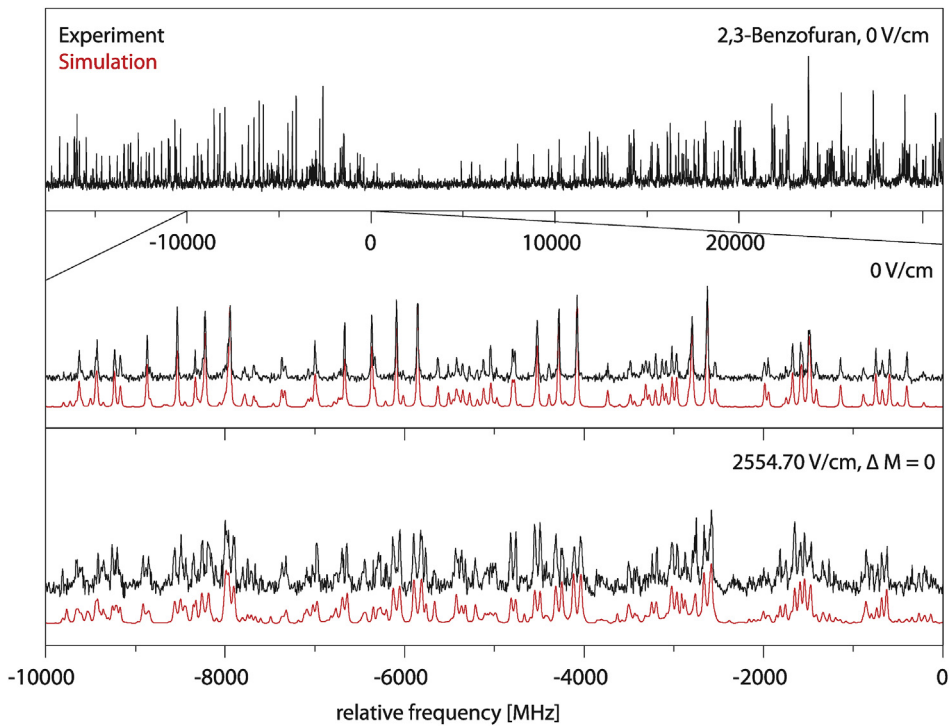


Fig. 3. Rotationally resolved electronic spectrum of the electronic origin of 2,3-benzofuran, along with a simulation with the best CMA-ES fit parameters.

vibrational effect, which is larger in the S_1 state.

For the fused system of benzene with 1,3-dioxole (analogue to furan with two oxygen atoms) forming 1,3-benzodioxole, Thomas *et al.* showed that the inertial defects point to a vibrationally averaged non-planar structure in both electronic states [57]. Also for 1,4-benzodioxan (benzene, fused with 1,4-dioxan, a six-

membered ring with two oxygen atoms), a non-planar equilibrium structure was found [58]. What is the reason for the different behavior between these benzene fused oxygen heteroring systems? It is obviously the fact that benzofuran has one of the oxygen lone pairs in a sp^2 like orbital, which makes it impossible to overlap with the remaining π orbitals, leaving benzofuran with 10 π electrons,

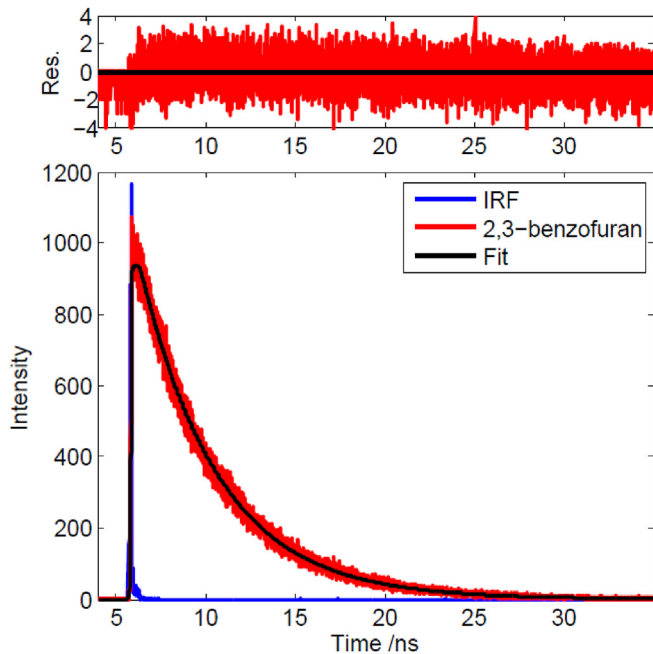


Fig. 4. TCSPC trace of 2,3-benzofuran in ethyl acetate solution, along with the instrument response function (IRF) and the best fit to a single exponential decay with excitation at 278 nm. Above, the residue of fit vs. experiment is shown.

which therefore is aromatic and planar. 1,3-benzodioxole and 1,4-benzodioxan also posses 10 π electrons, which, however are separated by one and two methylene bridges, respectively and are thus not conjugated.

The experimentally determined rotational constants of the excited state show a close agreement with the *ab initio* calculated values for the L_b-state, while those for the L_a-state show a larger deviation. Thus, already on the basis of the structural changes upon excitation, we have strong evidence that the excited state is of L_b-character.

If we compare the changes of the rotational constants to those of indole, we find a very close agreement. All rotational constants decrease upon electronic excitation, equivalent to an increase of the moments of inertia, pointing to an expansion of the molecules, which is in line with the assignment of the transition to be $\pi\pi^*$ in character. The geometry changes, which are expressed as rotational constant changes can be compared directly with each other, since the *pseudo* symmetry axis nearly coincides in both cases with the inertial *a*-axis. For excitation to the L_b-state a large decrease in the A rotational constant (-4%) is observed and calculated, accompanied by much smaller changes of B (-1%) and C (-2%) (cf. Table 2). Excitation to the L_a-state results in similar decrease of all three rotational constants. The same trend of changes between ground state and L_b- or L_a-state, respectively, is observed for indole.

Table 2
Comparison of the changes of the rotational constants of 2,3-benzofuran and indole upon electronic excitation.

molecule	2,3-benzofuran			Indole [14]		
	exp.	calc. L _b	calc. L _a	exp.	calc. L _b	calc. L _a
ΔA	-159.63	-164	-50	-134.75	-112	-28
ΔB	-15.39	-21	-36	-17.92	-27	-35
ΔC	-21.74	-25	-22	-20.73	-23	-19

4.2. Excited state lifetime

The excited state lifetime of 2,3-benzofuran (14.9 ns) in the gas phase is very close to that of indole (17.5 ns) [12,14,59,60]. The lifetime of 2,3-benzofuran in ethyl acetate solution is in general much shorter than in the gas phase. A single exponential decay with a lifetime of 4.4 ns is found. The fluorescence lifetime of green fluorescent protein (GFP) is on the order of a few nanoseconds [61]. Recent research takes place to replace the phenyl chromophore in GFP by 2,3-benzofuran in order to enhance the fluorescence [62]. Fluorescence lifetime measurements of the bare chromophore and in the liquid phase are therefore in need.

4.3. Dipole moments

4.3.1. Permanent dipole moments

The experimentally determined permanent dipole moment increases slightly from 0.77 D to 0.91 D (with an uncertainty of 0.01 D) in the excited singlet state with the angle of the dipole moment with the inertial *a*-axis which is nearly the same in the ground state (-72.7°) and the excited singlet state (-72.8°). If the permanent dipole moment in general is equal or smaller than in the electronic ground state it is a clear indication for an L_b-state. For an L_a-state there are in general comparatively large dipole moments.

A review about determination of dipole moments by Brown and Coller [63] reported an experimental value of 0.79 D from permittivity measurements in CS₂, close to the value we determined for the ground state of 2,3-benzofuran. The SCS-CC2/cc-pVTZ calculated value of 0.72 D is in excellent agreement with our experimental value. The direction of the dipole vector however shows larger deviations for the SCS-CC2/cc-pVTZ, than for the non spin component scaled CC2 variant. The excited state dipole moment increases by nearly 20% and has practically the same orientation as in the electronic ground state. Also for the excited state the agreement with the *ab initio* calculations is close. The calculated permanent dipole moment of the (experimentally not observed) L_a-state is nearly three times as high and oriented nearly perpendicular to the dipole moment of the L_b-state.

4.3.2. Transition dipole moments

The angle θ of the TDM can be determined to be $\pm 25.5^\circ$ (with an uncertainty of 2°) with respect to the inertial *a*-axis, in close agreement to the theoretical value of $+25.3^\circ$. We made the assignment of the sign of the TDM on the basis of the comparison to the *ab initio* calculated value. For indole, it was possible to determine the absolute value of the angle from an analysis of the relative signs of the axis reorientation angle θ_T and the TDM angle θ . However for 2,3-benzofuran, all band intensities can satisfactorily be reproduced using a rigid rotor Hamiltonian, while implementation of axis reorientation did not improve the fit of the rovibronic spectrum. From the *ab initio* optimized structures, the angle of reorientation of the inertial axis system upon electronic excitation θ_T can be determined using the relation for planar molecules given by Hougen and Watson [64]:

$$\tan(\theta_T) = \frac{\sum_i m_i (a_i' b_i'' - b_i' a_i'')}{\sum_i m_i (a_i' a_i'' + b_i' b_i'')} \quad (1)$$

Here, the doubly primed coordinates refer to the principal axis system in the electronic ground state and the singly primed quantities to the respective excited state inertial system and the m_i are the atomic masses. Using the SCS-CC2 optimized structures of the ground and electronically excited state, we obtain an axis reorientation angle of $+0.002^\circ$. The effect of such a small angles on

the band intensities is negligible, why inclusion of axis reorientation did not lead to an improvement of the fit. The respective angle in indole is 0.8° , nearly three orders of magnitude larger, hence it was possible to determine the absolute sign of θ in case of indol, but impossible for 2,3-benzofuran.

The orientation of the TDM vector away from the heteroatom in the furan moiety is the same as the orientation in indole with respect to the heteroatom of the pyran ring and hence can also be assigned to the orientation of an L_b -state. We did not observe bands that belong to the L_a -manifold. From the *ab initio* calculations we can see that the orientation of the L_a TDM is nearly perpendicular to that of the L_b . While these two states are nearly isoenergetic in case of indole, we have a gap of the adiabatic excitation energies of more than 5000 cm^{-1} making a vibronic coupling between the two lowest excited singlet states as in indole [14] extremely improbable.

5. Conclusion

Referring to the experimentally determined orientation of the transition dipole moment and the absolute values of the permanent dipole moments in the ground and excited state the lowest electronically excited singlet state of 2,3-benzofuran could be identified as an L_b -state. Also the geometry changes for excitation to the lowest excited singlet state are pointing to a L_b -like distortion of 2,3-benzofuran. Moreover the fluorescence lifetime in the gas phase could be determined from the Lorentzian contribution to the Voigt line profile using a fixed Gaussian contribution and compared to the excited state lifetime using TCSPC. The comparison to rotationally resolved electronic spectra of benzothiophene (the sulfur analogon of bezofuran) with respect to excited state lifetimes, which are currently on the way, will shed light on intersystem crossing in these aromatics.

Declaration of competing interest

The authors declare that they have no known competing financial interests or personal relationships that could have appeared to influence the work reported in this paper.

CRediT authorship contribution statement

Marie-Luise Hebestreit: Formal analysis, Investigation, Writing - original draft, Writing - review & editing, Visualization. **Hilda Lartian:** Investigation, Formal analysis. **Michael Schneider:** Investigation, Formal analysis. **Ralf Kühnemuth:** Resources. **América Yareth Torres-Boy:** Investigation. **Sergio Romero-Servin:** Investigation. **José Arturo Ruiz-Santoyo:** Investigation. **Leonardo Alvarez-Valtierra:** Investigation. **W. Leo Meerts:** Software. **Michael Schmitt:** Conceptualization, Methodology, Software, Supervision, Funding acquisition, Writing - original draft, Writing - review & editing.

Acknowledgements

Financial support of the Deutsche Forschungsgemeinschaft via grant SCHM1043/14-1 is gratefully acknowledged (M. S.). Financial support provided by CONACYT under the grant 277871 is greatly appreciated (L. A. V.). Computational support and infrastructure was provided by the "Center for Information and Media Technology" (ZIM) at the Heinrich-Heine-University Düsseldorf (Germany). We furthermore thank the Regional Computing Center of the University of Cologne (RRZK) for providing computing time on the DFG-funded High Performance Computing (HPC) system CHEOPS as well as support.

References

- [1] A.P. Antonella Liantonio, G. Carbonara, G. Fracchiolla, P. Tortorella, F. Loiodice, A. Laghezza, E. Babini, G. Zifarelli, M. Pusch, D.C. Camerino, Proc. Natl. Acad. Sci. U.S.A. 105 (2008) 1369–1373.
- [2] G. Ecker, W. Fleichhacker, T. Helm, C.R. Noe, S. Scasny, R. Lemmens-Gruber, C. Studenik, H. Marei, P. Heistracher, Chirality 6 (1994) 329–336.
- [3] A. Rickli, S. Kopf, M.C. Hoener, M.E. Liechti, Br. J. Pharmacol. 172 (2015) 3412–3425.
- [4] P.R. Callis, J. Chem. Phys. 95 (1991) 4230.
- [5] L.S. Slater, P.R. Callis, J. Phys. Chem. 99 (1995) 8572.
- [6] P.R. Callis, J.T. Vivian, L.S. Slater, Chem. Phys. Lett. 244 (1995) 53.
- [7] L. Serrano-Andrés, B.O. Roos, J. Am. Chem. Soc. 118 (1996) 185–195.
- [8] A.L. Sobolewski, W. Domcke, Chem. Phys. Lett. 315 (1999) 293–298.
- [9] A.C. Borin, L. Serrano-Andrés, Chem. Phys. 262 (2000) 253–265.
- [10] L. Serrano-Andrés, A.C. Borin, Chem. Phys. 262 (2000) 267–283.
- [11] C. Brand, J. Küpper, D.W. Pratt, W.L. Meerts, D. Krügler, J. Tatchen, M. Schmitt, Phys. Chem. Chem. Phys. 12 (2010) 4968–4979.
- [12] G. Berden, W.L. Meerts, E. Jalviste, J. Chem. Phys. 103 (1995) 9596–9606.
- [13] T.M. Korter, D.W. Pratt, J. Küpper, J. Phys. Chem. 102 (1998) 7211–7216.
- [14] J. Küpper, D.W. Pratt, W.L. Meerts, C. Brand, J. Tatchen, M. Schmitt, Phys. Chem. Chem. Phys. 12 (2010) 4980–4988.
- [15] D.M. Sammeth, S. Yan, L.H. Spangler, P.R. Callis, J. Phys. Chem. 94 (1990) 7340.
- [16] K.W. Short, P.R. Callis, J. Chem. Phys. 108 (1998) 10189–10196.
- [17] C. Brand, O. Oeltermann, D.W. Pratt, R. Weintraub, W.L. Meerts, W. van der Zande, K. Kleinermanns, M. Schmitt, J. Chem. Phys. 133 (2010), 024303–1–024303–11.
- [18] C. Brand, O. Oeltermann, M. Wilke, J. Tatchen, M. Schmitt, ChemPhysChem 13 (2012) 3134–3138.
- [19] C. Brand, O. Oeltermann, M. Wilke, M. Schmitt, J. Chem. Phys. 138 (2013), 024321.
- [20] J. Wilke, M. Wilke, W.L. Meerts, M. Schmitt, J. Chem. Phys. 144 (2016), 044201–1–044201–10.
- [21] M. Schneider, M.-L. Hebestreit, M.M. Lindic, H. Parsian, A.Y. Torres-Boy, L. Alvarez-Valtierra, W.L. Meerts, R. Kühnemuth, M. Schmitt, Phys. Chem. Chem. Phys. 20 (2018) 23441–23452.
- [22] O. Oeltermann, C. Brand, B. Engels, J. Tatchen, M. Schmitt, Phys. Chem. Chem. Phys. 14 (2012) 10266–10270.
- [23] T.B.C. Vu, I. Kalkman, W.L. Meerts, Y.N. Svartsov, C. Jacoby, M. Schmitt, J. Chem. Phys. 128 (1–8) (2008) 214311.
- [24] C. Brand, B. Happe, O. Oeltermann, M. Wilke, M. Schmitt, J. Mol. Struct. 1044 (2013) 21–25.
- [25] J. Wilke, M. Wilke, C. Brand, W.L. Meerts, M. Schmitt, ChemPhysChem 17 (2016) 2736–2743.
- [26] J. Wilke, M. Wilke, C. Brand, D. Spiegel, C. Marian, M. Schmitt, J. Phys. Chem. 121 (2017) 1597–1606.
- [27] M.-L. Hebestreit, M. Schneider, H. Lartian, V. Betz, M. Heinrich, M. Lindic, M.Y. Choi, M. Schmitt, Phys. Chem. Chem. Phys. 21 (2019) 14766–14774.
- [28] J.R. Platt, J. Chem. Phys. 17 (1949) 484–495.
- [29] G. Weber, Biochem. J. 75 (1960) 335–345.
- [30] Y. Yamamoto, J. Tanaka, Bull. Chem. Soc. Jpn. 45 (1972) 1362–1366.
- [31] J.M. Hollas, Spectrochim. Acta 19 (1963) 753–767.
- [32] A. Hartford, A.R. Muirhead, J.R. Lombardi, J. Mol. Spectrosc. 35 (1970) 199.
- [33] W.T. Yip, D.H. Levy, Jpc 100 (1996) 11539–11545.
- [34] J.T. Yi, L. Alvarez-Valtierra, D.W. Pratt, J. Chem. Phys. 124 (2006) 244302–244307.
- [35] L. Alvarez-Valtierra, J.T. Yi, D.W. Pratt, J. Phys. Chem. 113 (2009) 2261–2267.
- [36] W.B. Collier, J. Chem. Phys. 88 (1988) 7295–7306.
- [37] T.D. Klots, W.B. Collier, Spectrochim. Acta 51 (1995) 1291–1316.
- [38] T.L. Smithson, R.A. Shaw, H. Wieser, J. Chem. Phys. 81 (1984) 4281–4287.
- [39] M.H. Palmer, S.M.F. Kennedy, J. Chem. Soc. Perkin. Trans. 2 (1974) 1893–1903.
- [40] S. Gerstenkorn, P. Luc, Atlas du spectre d'absorption de la molécule d'iode 14800–20000 cm^{-1} , CNRS, Paris, 1986.
- [41] M. Schmitt, Habilitation, Heinrich-Heine-Universität, Math. Nat. Fakultät (2000), Düsseldorf.
- [42] M. Schmitt, J. Küpper, D. Spangenberg, A. Westphal, Chem. Phys. 254 (2000) 349–361.
- [43] K. Wohlfart, M. Schnell, J.U. Grabow, J. Küpper, J. Mol. Spectrosc. 247 (2014) 119–121.
- [44] R. Ahlrichs, M. Bär, M. Häser, H. Horn, C. Kölmel, Chem. Phys. Lett. 162 (1989) 165–169.
- [45] J.T.H. Dunning, J. Chem. Phys. 90 (1989) 1007–1023.
- [46] C. Hättig, F. Weigend, J. Chem. Phys. 113 (2000) 5154–5161.
- [47] C. Hättig, A. Köhn, J. Chem. Phys. 117 (2002) 6939–6951.
- [48] C. Hättig, J. Chem. Phys. 118 (2002) 7751–7761.
- [49] A. Hellweg, S. Grün, C. Hättig, Phys. Chem. Chem. Phys. 10 (2008) 1159–1169.
- [50] P. Deglmann, F. Furche, R. Ahlrichs, Chem. Phys. Lett. 362 (2002) 511–518.
- [51] W.L. Meerts, M. Schmitt, G. Groenenboom, Can. J. Chem. 82 (2004) 804–819.
- [52] W.L. Meerts, M. Schmitt, Phys. Scripta 73 (2005) C47–C52.
- [53] W.L. Meerts, M. Schmitt, Int. Rev. Phys. Chem. 25 (2006) 353–406.
- [54] M. Schmitt, W.L. Meerts, in: M. Quack, F. Merkt (Eds.), Handbook of High Resolution Spectroscopy, John Wiley and Sons, 2011.
- [55] A. Ostenmeier, A. Gawelcyk, N. Hansen, in: Y. Davidor, H.-P. Schwefel, R. Männer (Eds.), Parallel Problem Solving from Nature, PPSN III, Springer,

- Berlin/Heidelberg, 1994.
- [56] N. Hansen, A. Ostermeier, *Evol. Comput.* 9 (2001) 159–195.
- [57] J.A. Thomas, L. Alvarez-Valtierra, D.W. Pratt, *Chem. Phys. Lett.* 490 (2010) 109–115.
- [58] T.B.C. Vu, C. Brand, W.L. Meerts, M. Schmitt, *ChemPhysChem* 12 (2011) 2035.
- [59] J.W. Hager, S.C. Wallace, *J. Phys. Chem.* 87 (1983) 2121.
- [60] G.A. Bickel, D.R. Demmer, E.A. Outhouse, S.C. Wallace, *J. Chem. Phys.* 91 (1989) 6013.
- [61] G. Striker, V. Subramaniam, C.A.M. Seidel, A. Volkmer, *J. Phys. Chem. B* 103 (1999) 8612–8617.
- [62] M.A. Christensen, K. Jenum, P.B. Abrahamsen, E.A.D. Pia, K. Lincke, S.L. Broman, D.B. Nygaard, A.D. Bond, M.B. Nielsen, *RSC Adv.* 2 (2012), 8273–8249.
- [63] R.D. Brown, B.A.W. Coller, *Theor. Chim. Acta* 7 (1967) 259–282.
- [64] J.T. Hougen, J.K.G. Watson, *Can. J. Phys.* 43 (1965) 298–320.